

## RESEARCH ARTICLE

10.1002/2013JC009668

## Key Points:

- Identification of storms footprints to form homogeneous regions
- Estimation of extreme significant wave heights with regional frequency analysis
- Procedure to extract storms generating marine extremes

## Correspondence to:

J. Weiss,  
jerome.weiss@edf.fr

## Citation:

Weiss, J., P. Bernardara, and M. Benoit (2014), Formation of homogeneous regions for regional frequency analysis of extreme significant wave heights, *J. Geophys. Res. Oceans*, 119, 2906–2922, doi:10.1002/2013JC009668.

Received 27 NOV 2013

Accepted 18 APR 2014

Accepted article online 21 APR 2014

Published online 14 MAY 2014

## Formation of homogeneous regions for regional frequency analysis of extreme significant wave heights

Jérôme Weiss<sup>1,2</sup>, Pietro Bernardara<sup>1,3</sup>, and Michel Benoit<sup>1,2</sup>

<sup>1</sup>Saint-Venant Hydraulics Laboratory (ENPC, EDF R&D, CEREMA), Université Paris-Est, Chatou, France, <sup>2</sup>EDF R&D Laboratoire National d'Hydraulique et Environnement, Chatou, France, <sup>3</sup>EDF Energy R&D UK Centre, London, UK

**Abstract** Regional frequency analysis (RFA) can reduce uncertainties in the estimations of return levels, provided that homogeneous regions can be delineated. In the framework of extreme marine events, a physically based method to form homogeneous regions by identifying typical storms footprints is proposed. First, a spatiotemporal declustering procedure is employed to detect storms generating marine extremes. Second, the identification of the most typical storms footprints relies on a clustering algorithm based on a criterion of storm propagation. The resulting regions are readily explicable: sites from a given region are likely to be impacted by the same storms, and any storm impacting a region is likely to remain enclosed in this region. This procedure is fairly simple to implement, as the only information required is the time of occurrence of the observed extremes. An application to the estimation of extreme significant wave heights from the numerical sea-state database ANEMOC-2 is given. Six regions, both physically and statistically homogeneous, are delineated in the North-East part of the Atlantic Ocean. It is shown that the identification of storms footprints allows the increase of the overall statistical homogeneity. Combined with RFA, the proposed method highlights regional differences in the spatial extent and intensity of storms.

### 1. Introduction

Coastal engineering inevitably deals with extreme marine hazards. For instance, the design of effective coastal protections needs accurate estimations of extreme quantiles of sea levels or wave heights. These quantities are traditionally obtained by a local statistical analysis, from a time series observed at a given site. However, local durations of observations may be too low to accurately estimate return levels.

If data from several sites of observations are available, some methods exist to reduce these uncertainties. For example, the parameters of the distribution of extremes can be assumed to smoothly vary in space, through a latent spatial process [Casson and Coles, 1999; Davison *et al.*, 2012]. Another possible way is to perform a regional frequency analysis (RFA) based on the index flood method popularized by Dalrymple [1960]. The main idea is to exploit the information from similar sites in a region, by assuming a common extremal behavior in the region. In particular, RFA assumes that observations from sites coming from a homogeneous region follow the same regional probability distribution, up to a local index representing the local specificities of a site.

In particular, the step of grouping sites into regions is essential, as it defines how the regional information is exploited and thus can deeply influence the final results. Several hydrological studies considered this question, which remains open. Sites can be grouped according to their geographical proximity. For instance, Beable and Mckerchar [1982] divided New Zealand into nine administrative regions to estimate floods. A proper understanding of the mechanisms generating the variable of interest can also lead to physically homogeneous regions. To study streamflows in Ontario and Quebec, Gingras *et al.* [1994] pooled sites according to the time of year when extreme floods are usually observed. Unsupervised learning methods are also useful to group sites according to their similarities. For instance, annual maxima precipitation in Quebec were considered by Onibon *et al.* [2004] who used hierarchical ascendant clustering on mean annual rainfalls to form regions. Ramachandra Rao and Srinivas [2006] used a hybrid of Ward's and *k*-means algorithms to perform a RFA of watersheds in Indiana, USA, where homogeneous regions are found by grouping sites according to the similarities between catchments. Factor analysis, where sites are grouped when their corresponding variability is explained by the same factor axis, is another possibility. Morin *et al.* [1979] employed principal component analysis to form regions in order to study precipitations in Quebec.

In the hydrological literature, the formation of homogeneous regions is thus generally carried out from statistics related to the variable of interest, and/or from explicative variables physically linked to the variable of interest. *Gabriele and Chiaravalloti* [2013] and *Satyanarayana and Srinivas* [2008] argue in favor of using meteorological information to improve the formation of homogeneous regions. In principle, whatever the method used, the partition should be validated by tests of statistical homogeneity, such as those proposed by *Hosking and Wallis* [1993].

Fewer applications of RFA can be found in the literature to characterize extreme marine hazards. *Bernardara et al.* [2011] and *Bardet et al.* [2011] analyzed extreme skew storm surges along the French coasts of the Atlantic Ocean and the English Channel for 21 and 18 sites, respectively. This area is statistically homogeneous according to the Hosking and Wallis test. *Van Gelder et al.* [2000] used a similar argument to regionalize extreme wave heights from nine sites located in the North Sea, forming a homogeneous region after computation of the Hosking and Wallis test. To perform another RFA of extreme wave heights, *Goda et al.* [2010] and *Goda* [2011] proposed to group 11 sites located along the eastern coast of Japan sea into two homogeneous regions (North or South). This partitioning is due to the fact that the whole area is not homogeneous in the sense of the Hosking and Wallis test. Sites are thus assigned in one region according to their latitude, and the separation between the two regions is made so that the Hosking and Wallis test validates the partition.

These studies were carried out in relatively statistically homogeneous areas, which is not always the case when dealing with marine hazards. The analysis of extreme sea levels from *Van Gelder and Neykov* [1998] showed the heterogeneity of the region made of 13 sites of the North Sea coast of the Netherlands. A possible explanation of this heterogeneity could be that these sites are either located in open seas or in estuarine areas, or are protected by islands. They would be under the influence of different physical processes, indicating that a statistical heterogeneity would be a consequence of a physical heterogeneity.

Very few marine studies tried to rely on physical arguments to form homogeneous regions. For instance, in order to estimate extreme skew storm surges for 16 sites along the coasts of the United Kingdom, *Weiss and Bernardara* [2013] have divided the study area into two homogeneous regions according to the coastal orientation (South or West). Moreover, to study tsunami runup height, *Hosking* [2012] grouped 114 sites of the Pacific Ocean into 10 homogeneous regions. This partitioning is based on both the geographical distance and the similarities between at-site coefficients of variation. This sense of geographical coherence is a first step toward a nonpurely statistical grouping. However, *Hosking* [2012] suggests it would be even more relevant to consider the coastal exposure in relation to the different type of events generating the observed extremes, as well as their typical trajectories. Yet such a procedure could require much supporting information, which is not always easily available.

Thus, no method dedicated to marine hazards was formalized to build homogeneous regions. Indeed, through this bibliographical review, there are generally only few, if not none, physical considerations behind the formation of regions, the latter being usually justified as soon as the Hosking and Wallis test do not reject the statistical homogeneity. Thus, the resulting groupings are either arbitrary or purely statistical. In that case, they are not easily explicable: *Kergadallan* [2013] noticed that statistical tests of homogeneity fail to reject estuarine areas, where fluvial inputs influence the observed sea level. Moreover, their generalization to similar problems (adding a site in the region, study of other sites in the same area, analysis of another variable sensitive to the same physical processes, etc.) may not be immediate. Besides, as suggested by *Van Gelder and Neykov* [1998], a statistical heterogeneity may be explained by physical reasons. In other words, a physically homogeneous region would be a good candidate to be also a statistical homogeneous region.

In this framework, the general objective of this paper is to propose a physically based method to form homogeneous regions for RFA of extreme marine events.

The introduced approach is based on the identification of typical storms footprints. Sites are gathered into different regions, according to their location in relation to storms footprints. Thus, sites from a given region would be likely to be impacted by the same storms, indicative of a regional physical homogeneity. Moreover, as any storm impacting a region would be likely to remain enclosed in this region, different types of storms could be identified in the study area: we can expect the probabilistic behavior of extremes to vary between regions. For this purpose, a clustering algorithm based on a criterion of storm propagation is

introduced in this paper. Note that, as highlighted by *Hosking* [2012], the definition of physical homogeneity may be linked to an important and complicated processing of several external variables, which can limit the use of such an approach. However, the proposed method is not computationally expensive since it does not require any other information than the time of occurrence of the observed extremes.

Clustering procedures allow to group objects into different clusters based on a similarity measure. These clusters have to be compact (objects are similar within a cluster) and well separated (clusters are distinct from each other). In the framework of synoptic climatological classification, *Michelangeli et al.* [1995] used the *k*-means algorithm to determine recurrent weather regimes over the Atlantic and Pacific regions; *Holt* [1999] classified atmospheric conditions under which extreme storm surges are generated in the Irish Sea and the North Sea with factor analysis; *Betts et al.* [2004] used Ward's hierarchical clustering method to identify six cyclone track regimes causing extreme storm surges at Brest, France. Ward's clustering algorithm [*Ward*, 1963] is well known. According to *Everitt and Dunn* [2001], it implies that the dispersion within (between) clusters is minimized (maximized). This method generally performs well to accurately find clusters [*Blashfield*, 1976; *Ferreira and Hitchcock*, 2009; *Modarres and Sarhadi*, 2011]. However, a possible disadvantage is its tendency to form regions of roughly equal size, which can, for instance, be debatable when dealing with synoptic climatological classification [*Kalkstein et al.*, 1987].

The tracking of cyclones often relies on a proper nearest-neighbor search in space and time, "partly taking into account an expected movement of a cyclone according to a consideration of flow dynamics and of previous motion of the system" [*Ulbrich et al.*, 2009]. Thus, both the definition and the extraction of storms require a particular care. Spatiotemporal declustering procedures are usually used to track storms, while taking into account their propagation in space and time. For example, by linking storm severity and surface wind speed, *Leckebusch et al.* [2008], *Nissen et al.* [2010], and *Renggli et al.* [2010] identified storms from spatiotemporally coherent exceedances of a high quantile of wind speed distribution. In this paper, such an approach is adapted to marine hazards.

RFA assumes that observations at different sites are independent. As a same storm is likely to impact several sites, this is rarely verified in reality. A possible way to come down to this hypothesis is to filter observations stemming from the same storms. However, according to *Kergadallan* [2013], the definition of such a filter should be based on a proper knowledge of the propagation of atmospheric depressions. For example, to estimate extreme skew storm surges at different sites, *Bernardara et al.* [2011] and *Bardet et al.* [2011] removed any spatial dependence through a declustering procedure by keeping the highest observation among extremes occurring within 72 h. However, this filter neither allows separation of different storms occurring simultaneously in different areas, nor distinction of serial clustering of storms, such as the Lothar and Martin storms of December 1999 [*Mailier et al.*, 2006]. Thus, the extraction of storms should be able to identify at best the different physical events propagating in space and time.

The procedure to extract storms is explained in section 2.1, and the new proposed method to form homogeneous regions is presented in section 2.2. Sections 2.3–2.5 are dedicated to the estimation of extreme quantiles by RFA. An illustration with significant wave heights from the numerical database ANEMOC-2 is given in section 3.

## 2. Methodology

### 2.1. Extraction of Storms

The storm tracking is usually a complex task. Indeed, from the representation of spatiotemporal profiles of storms near the UK coasts of the North Sea, *Butler* [2005] showed the difficulty to provide a statistically clear definition of North Sea storms, because of their great variability. Moreover, *Anderson et al.* [2001] noted that "wave fields associated with each storm do not always form a single coherent cell, the areas of high waves fragment and almost disappear before reforming and regaining strength on the following morning." The extraction of storms should be able to take into account both the variability of storms dynamics and their possible nonuniform propagation.

In this paper, storms are directly characterized through the marine variable of interest. A storm is defined as a physical event generating marine extremes in at least one site in the study area. For a given site, an observation is characterized as extreme if it exceeds  $q_p$ , the *p*-quantile of the initial time series. A storm thus

impacts this site if  $q_p$  is exceeded. It indicates if each site is impacted. Given that at least one site is impacted by a storm, information on its impact on each site is provided. Storms are therefore purely statistical objects, providing information on the spatial extent of the extremes generated.

As storms propagate in space and time, their detection is based on a spatiotemporal declustering procedure. The main principle is that extremes neighbors in space and time are supposed to be part of the same storm. Specifically, two extremes are spatiotemporal neighbors if (i) they occurred within  $\Delta$  hours and (ii) they are among the  $\eta$ -nearest neighbors of each other.

We provide a more precise description of the extraction of storms. At a given time, let a spatial cluster be the collection of sites neighbors in space impacted by a same storm. It can be detected by representing the study area by a graph where nodes represent sites. Each site is initially connected to its  $\eta$ -nearest neighbors. Connections from sites which are not impacted by the current storm are then removed, and the remaining connections determine one or more spatial clusters. Next, two spatial clusters A and B are said to be spatial (temporal) neighbors if at least one site of A is among the  $\eta$ -nearest neighbors of any site of B (they occurred within  $\Delta$  hours). Finally, spatial clusters which are both spatial and temporal neighbors are merged, as they are supposed to stem from the same storm.

A storm may cross land areas and impact two different, but relatively near, coasts. For example, the Xynthia storm of February 2010 generated extreme skew storm surges both on the Bay of Biscay French coasts and on the Albâtre coast (Haute-Normandie, France). In that case, to ensure that the algorithm detects only one storm, connections between coastal sites are added in the  $\eta$ -nearest neighbor graph, for coasts being likely to be part of the same storm track (such as the French coasts or islands like UK, Ireland, or Iceland). Hence, the  $\eta$ -nearest neighbors approach can carefully detect such storms, unlike a classical intersite geographical distances approach.

Three parameters are thus required to detect a storm:  $p$ , setting its impact on a given site, and  $(\Delta, \eta)$  which are related to its spatiotemporal propagation.  $(p, \Delta, \eta)$  should be chosen in order to guarantee a proper detection of these physical events. If  $p$  is too high and  $\Delta$  or  $\eta$  is too low, it is likely that a same physical event will be wrongly separated into two or more storms. Conversely, if  $p$  is too low and  $\Delta$  or  $\eta$  is too high, it is likely that two distinct storms may be wrongly merged. Besides, note that the concept of spatial clusters allows separating different events occurring simultaneously in different areas; moreover,  $\Delta$  plays a role to detect storms occurring in serial clusters. Furthermore, as mentioned above, possible nonuniform storm propagation can be taken into consideration through a proper definition of  $(p, \Delta, \eta)$ . Finally, the spatiotemporal neighborhood relationship implied by  $(\Delta, \eta)$  needs to be carefully defined, for example, according to the spatiotemporal resolution of observations, the possible missing values and the physical propagation of the considered phenomenon. This procedure leads to define storms as spatiotemporally coherent exceedances of the  $p$ -quantile at site scale. *Leckebusch et al.* [2008], *Nissen et al.* [2010], and *Renggli et al.* [2010] used a similar approach to detect storms from wind speed observations. In particular, it is assumed that this declustering procedure provides a sample of  $S$  independent storms.

## 2.2. Formation of Physically Homogeneous Regions

The objective is to propose a physically based method to form homogeneous regions, by identifying the typical storms footprints in the study area. The set of sites must be partitioned in such a way that each resulting group represents a typical storm impact area. This can be achieved through the development of a clustering algorithm based on a criterion of storm propagation.

Assuming  $N$  sites in the study area where  $S$  storms are observed, let  $Z_s^i$  be the Bernoulli variable which is one if site  $i$  is impacted by a storm  $s$ . We define a criterion of storm propagation  $p_{i,j}$  as the probability that both sites  $i$  and  $j$  are impacted by a storm given that one of them is:

$$p_{i,j} = P(Z_s^i = 1, Z_s^j = 1 \mid Z_s^i + Z_s^j \geq 1) \tag{1}$$

These probabilities are estimated for each possible pair of sites  $(i, j)$ , from the sample of storms. Then, a dissimilarity index defined as:

$$d_{i,j} = 1 - p_{i,j} \tag{2}$$

is computed for each pair of sites. In particular, if  $d_{ij} = 0$ , then any storm impacting  $i$  or  $j$  necessarily hits the other; conversely, if  $d_{ij} = 1$ , then any storm impacting  $i$  or  $j$  necessarily avoids the other. Note that (1) and (2) are reformulations of the Jaccard index and the Jaccard distance, respectively.

The next step is to group all sites into  $R$  disjoint regions, according to their similarity in terms of (2). As the classification is made directly from the criterion of storm propagation (1), the resulting partition can be considered to represent storms footprints. Ward's hierarchical clustering algorithm [Ward, 1963] is employed here. It is generally intended for Euclidean distances, but Cao *et al.* [1997] showed it can properly perform even when non-Euclidean distances are used. As the dissimilarities (2) are not Euclidean, the extension of Ward's method for an arbitrary dissimilarity measure provided by Mirkin [2005] is applied. In particular, distances between clusters coincide with the usual Ward's distance when using Euclidean squared distances. This is an agglomerative hierarchical method: (i) each site is initially assigned to its own region and (ii) the closest pair of regions is merged until there is only one region. The resulting hierarchy of regions can be represented in a dendrogram. However, as non-Euclidean dissimilarities are used, the heights of the dendrogram do not express the distance between groups in terms of (2). Note that hierarchical clustering is preferred here to a strict partitioning clustering (such as the  $k$ -means algorithm), because the obtained hierarchical structure allows to refine the physical interpretation of the regions. Indeed, the possibility to subdivide a given region may help to understand how the storms footprints are organized.

For fixed  $R$ , the study area is thus partitioned in  $R$  regions. Among the different configurations of storms footprints obtained when varying  $R$ , the objective now is to determine the most relevant one. The optimal number of regions can be determined with an index measuring the goodness of a clustering. A proper partition should contain well-separated regions, with sites close to each other inside a given region (compactness), in terms of (2). For instance, Mojena's stopping rule [Mojena, 1977] attempts to find the level in the hierarchy implying a significant jump in the dendrogram heights, indicative of the merging of two dissimilar clusters. This strategy was, for example, used by Yun and Cho [2006] to conclude that quality of fingerprint images could be grouped into five clusters. However, Martinez and Martinez [2004] remarked the significance of a jump is not straightforward to assess; they recommended instead the visual inspection of a break in the evolution of the standardized dendrogram heights in function of the number of clusters.

The proper number of regions is thus determined through the latter procedure, leading to the identification of the most typical storms footprints. Specifically, a storm impacting a given region is likely to remain enclosed in this region, and sites in this region are likely to be impacted by the same storms.

### 2.3. Preparation of Samples for Statistical Analysis

At a given site, RFA requires that observations are independent; yet, several successive extremes can be generated by a same storm. The traditional "peaks over threshold" (POT) method usually imposes that two storm events can be considered independent if there is a certain time lag between them. It should be mentioned that this parameter is not required here, as  $\Delta$  suffices to get independent storms at site scale, see section 2.1. In particular, when a storm lasts long enough to generate several extremes, only the peak value is retained to summarize this storm while obtaining independent extremes at site scale. The maximum value recorded during the storm  $s$  impacting site  $i$  is denoted by  $W_s^i$ .

Storms from section 2.1 are extracted in order to decluster physical events while reproducing as well as possible their spatiotemporal dynamics, and are used to form physically homogeneous regions. However, this step can be distinguished from statistical aspects, such as testing the statistical regional homogeneity or the goodness-of-fit in the upper tails of distributions. This "double-threshold" approach is recommended in Bernardara *et al.* [2014] to deal with auto-correlated environmental variables in a POT framework. The principle is to (i) identify independent events (where the variable is notably out of its mean regime) through a *physical* threshold and (ii) from these events, find a *statistical* threshold leading to a proper estimation of extreme quantiles. Thus, for statistical aspects covered in sections 2.4 and 2.5, only the most intense events are considered. New thresholds, denoted  $u$  and higher than the quantiles  $q_p$ , are selected corresponding to the observation of  $\lambda$  storms per year on average at each site. In particular at site  $i$ , if  $d_i$  years of data are available, the  $n_i = \lambda d_i$  highest  $W_s^i$  are retained in the final  $n_i$ -sample  $X^i$ . The threshold  $u_i$  exceeded on average  $\lambda$  times per year is then defined as the smallest observation of  $X^i$  (minus an infinitesimal quantity). Storms are then statistically redefined: if site  $i$  was impacted by storm  $s$ , it is from now on impacted by  $s$  if and only if  $u_i$  is exceeded.

The choice of  $\lambda$  is the consequence of a trade-off between variability and bias of the final quantile estimates. In local analyses, for example, the value  $\lambda = 1$  generally results in too small samples, leading to a high variability in the estimates. However, in a RFA framework, *Bernardara et al.* [2011] used  $\lambda = 1$ . Indeed, as data from several sites are simultaneously considered, a focus can be made on the most extreme observations, reducing thus the bias in the final estimates, but without implying a high variability.  $\lambda = 1$  is therefore chosen in the following of this study.

#### 2.4. Statistical Homogeneity of the Obtained Regions

Statistically homogeneous regions are required to perform RFA. Although section 2.2 allows delineating physically homogeneous regions, their statistical homogeneity must be checked.

Discordant sites within a given region can be identified through the discordancy criterion  $D$  of *Hosking and Wallis* [1993]. It measures if a given site is significantly different from all the other sites in the region, in terms of  $L$ -moments. A site can be declared discordant if  $D > 3$  for regions with more than 15 sites. Moreover, the degree of statistical homogeneity of a candidate region can be evaluated with the criterion proposed by *Hosking and Wallis* [1993]. Their heterogeneity measure  $H$  indicates whether the observed dispersion between sites is comparable to what would be expected in a statistically homogeneous region. In particular, the region can be considered as statistically homogeneous if  $H < 2$ , and heterogeneous otherwise. However, this rule was originally derived for regions with no intersite dependence. Here regions correspond to storms footprints and a strong intersite dependence can thus be expected. In section 3.5, it is shown that the criterion  $H = 2$  remains valid to detect heterogeneity in such regions.

Thus, for each storm footprint, the following process is applied:

1. Computation of the heterogeneity measure  $H$  from the samples  $X^i$ . If  $H < 2$  then go to (iv), else go to (ii).
2. Computation of the discordancy measures  $D$  from the samples  $X^i$ . If no site is discordant then go to (iii), else remove the sites with  $D > 3$  and compute a new heterogeneity measure  $H'$ . If  $H' < 2$  then go to (iv), else go to (iii).
3. Subdivision of the region into two new regions stemming from the classification of section 2.2. For each subregion, go to (i).
4. The region is both physically and statistically homogeneous.

This procedure yields both physically and statistically homogeneous regions, and RFA can then be performed. Note that, even if a region is statistically homogeneous, it is worth checking for discordant sites (e.g., if error measurement is present in the data). However, if a particular area is subdivided several times without improving statistical homogeneity, it is possible to retain a subdivision as a compromise between a low statistical heterogeneity and a sufficient number of sites in the region, while interpreting the results from RFA with care. In that case, a local statistical analysis may be preferable: even if estimates may have a high variability, they should be relatively unbiased.

#### 2.5. Regional Frequency Analysis

The methodology presented in this paper requires handling exceedances over a high threshold. From the extreme value theory, these exceedances can be modeled with the Generalized Pareto Distribution (GPD) [*Pickands, 1975*]. For site  $i$ , let  $u_i$  be the storm threshold which is exceeded on average  $\lambda$  times per year (see section 2.3). The  $n_T$ -sample  $X^i$ , denoting the exceedances of  $u_i$ , is assumed to be drawn from a GPD:  $X^i \sim \text{GPD}(u_i, \alpha_i, k_i)$ , where  $\alpha_i > 0$  and  $k_i$  are, respectively, a scale and a shape parameter. In particular, the  $p$ -quantile of  $X^i$  is:

$$x_p^i = \begin{cases} u_i - \alpha_i / k_i (1 - (1 - p)^{-k_i}), & k_i \neq 0 \\ u_i - \alpha_i \log(1 - p), & k_i = 0 \end{cases} \quad (3)$$

The right tail of the GPD is bounded when  $k_i < 0$ , and unbounded when  $k_i \geq 0$ . The  $T$ -year return level, i.e., the value exceeded on average once every  $T$  years, is given by  $x_{1-1/\lambda T}^i$  [*Rosbjerg, 1985*].

RFA based on the index flood method [*Dalrymple, 1960*] relies on a homogeneity hypothesis; observations from sites coming from a homogeneous region are supposed to follow the same regional probability

distribution, up to a local index representing the local specificities of a site. For a homogenous region of  $N$  sites, let  $\mu_i$  be the local index of the site  $i = 1, \dots, N$ . By the regional homogeneity hypothesis, the distribution of the normalized variable  $Y^i = X^i/\mu_i$  is supposed to be independent of  $i$ .

The local index  $\mu_i$  is often taken as the mean value of the at-site observations; furthermore, Weiss and Bernardara [2013] have shown that choosing other indices could worsen the performances of the RFA. However, Roth et al. [2012] showed that dealing with exceedances over a high threshold necessarily implies that the local index has to be a multiple of this threshold. Here  $\mu_i$  is therefore chosen as the storm threshold  $u_i$ . This implies that  $Y^i \sim \text{GPD}(1, \gamma, k)$ , where: (i) the regional scale parameter satisfies  $\gamma = \alpha_i/u_i$  and (ii) the shape parameter  $k_i = k$  is constant over the region. From these relationships,  $X^i \sim \text{GPD}(u_i, \gamma u_i, k)$ .

The two regional parameters  $(\gamma, k)$  can be estimated with the regional  $L$ -moments method depicted by Hosking and Wallis [1997]. Let  $\hat{\lambda}_r^i$  be the sample  $r$ -order  $L$ -moment for site  $i$ ; the sample regional  $r$ -order  $L$ -moment is  $\hat{\lambda}_r^R = \sum_{i=1}^N n_i(\hat{\lambda}_r^i/u_i) / \sum_{i=1}^N n_i$ . Then,  $(\gamma, k)$  are estimated as follows:

$$\hat{k} = 2 - (\hat{\lambda}_1^R - 1) / \hat{\lambda}_2^R, \quad \hat{\gamma} = (1 - \hat{k})(\hat{\lambda}_1^R - 1) \tag{4}$$

Note that, for a GPD distributed variable, theoretical  $L$ -moments exist for  $k < 1$ . For site  $i$ , the  $T$ -year return level is obtained by multiplying the regional  $T$ -year return level by the local index:  $x_{1-1/\lambda T}^i = u_i y_{1-1/\lambda T}$ .

RFA assumes that observations at different sites are independent. However, as sites in a region are likely to be impacted by the same storms, a strong intersite dependence is expected. The regional  $L$ -moments method is still used here, as it was shown to be quite robust to the presence of intersite dependence [Hosking and Wallis, 1988]. Besides, although the GPD is here assumed, other candidate distributions can be tested and compared, for example, through the use of a regional  $L$ -moment ratio diagram.

### 3. Application

#### 3.1. Data Used

ANEMOC-2 (Atlas Numérique d'États de Mer Océaniques et Côtiers-Numerical Atlas of Oceanic and Coastal Sea states) is a numerical sea-state hindcast database covering the Atlantic Ocean over the period 1979–2009 (31 years). It has been developed at Saint-Venant Laboratory for Hydraulics and EDF R&D LNHE [Laugel, 2013]. The simulations of wave conditions have been carried out with the third-generation spectral wave

model TOMAWAC [Benoit et al., 1996] and have been forced by wind fields from the CFSR reanalysis database [Saha et al., 2010].

The spatial resolution of the so-called “oceanic mesh” of ANEMOC-2 ranges from about 120 km over the Northern part of the Atlantic Ocean down to about 20 km along the European coast and 10 km along the French coast. For the present study, a subset of 1847 nodes among the 13,426 nodes of the full oceanic mesh is selected, at locations plotted in Figure 1.

Among the wave parameters available with an hourly resolution in ANEMOC-2, we consider here the significant wave height, denoted  $H_s$ , which is the usually preferred parameter to

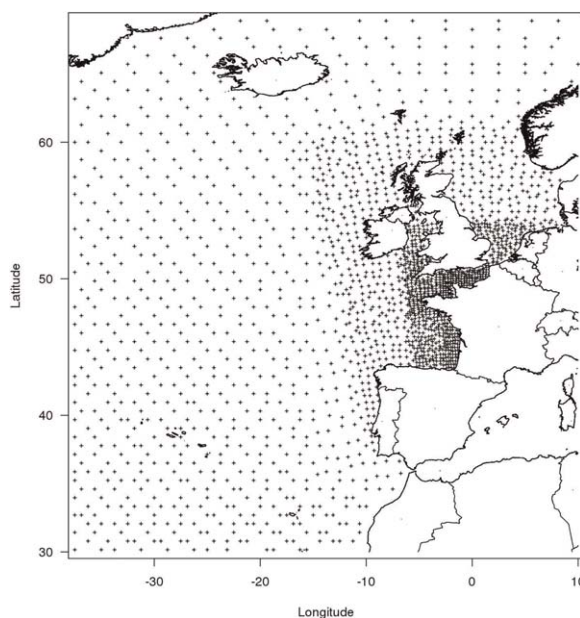


**Figure 1.** Location of the 1847 sites extracted from the oceanic mesh of the ANEMOC-2 sea-state database.

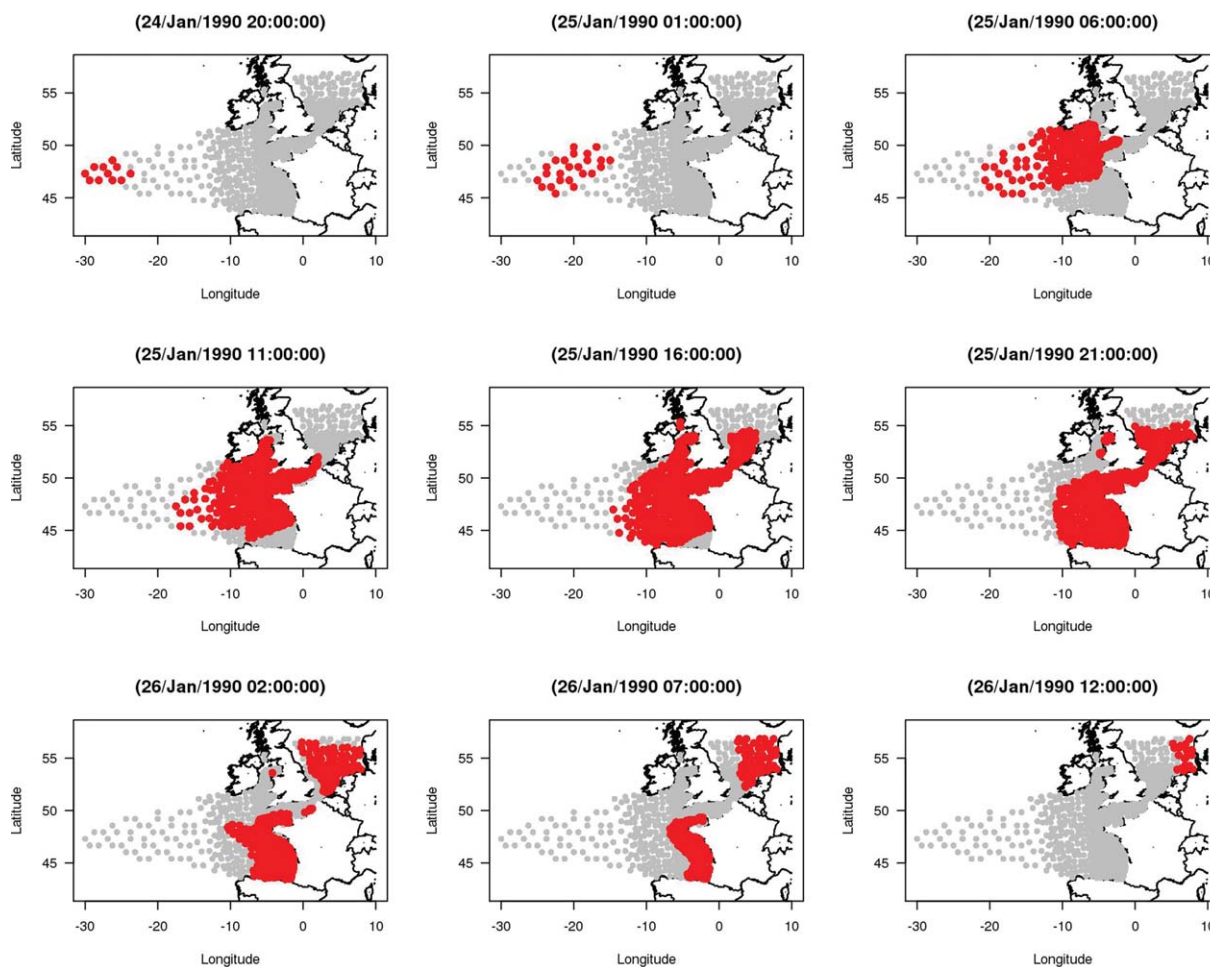


**Figure 2.** Storm Daria (24–26 January 1990): snapshot every 5 h, where red dots indicate the impacted sites (exceedances of the 0.995 quantile of hourly time series of  $H_s$ ) and gray dots represent the storm footprint.

summarize sea state conditions and intensity. TOMAWAC computes this wave height from the zero-order moment of the wave spectrum. Hourly series of significant wave heights  $H_s$  over the period 1979–2009 are

thus extracted for the 1847 selected sites. The objective here is to apply the methodology described in section 2 to form physically homogeneous regions by identifying typical storms footprints in this area and to estimate extreme significant wave heights by RFA.

### 3.2. Extraction of Storms

The parameters ( $p, \Delta, \eta$ ) defined in section 2.1 are set in order to faithfully reproduce the physical dynamics of the storms present in the database, while taking into account the spatiotemporal resolution of observations.

A particular attention should be paid to the choice of  $p$ . It is likely that proper values of  $p$  depend on the situation, as the storm dynamics may differ according to

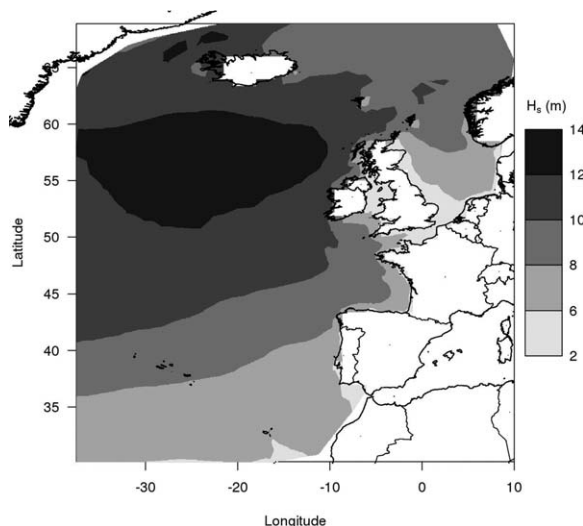


**Figure 3.** Map of 0.995 quantiles of hourly time series of  $H_s$  (m).

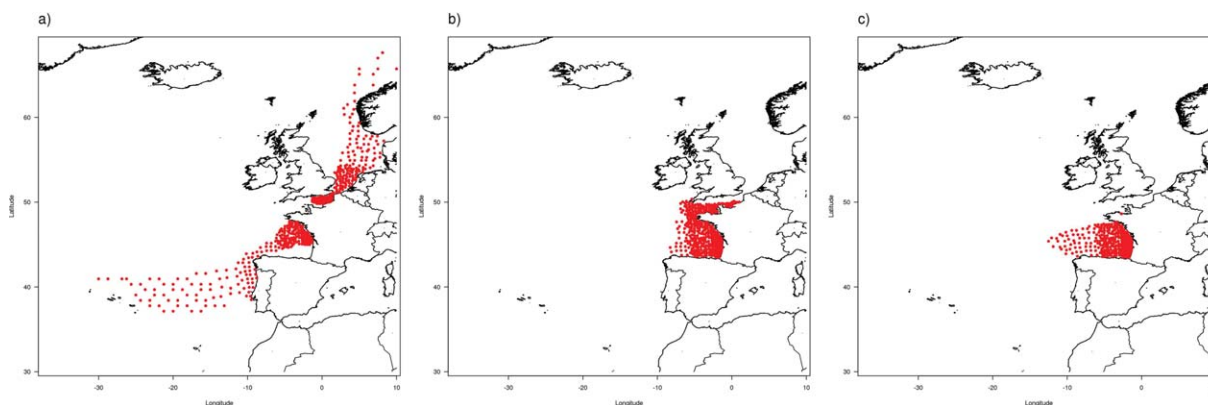


**Figure 4.** Footprints of (a) the Great Storm of 1987 (15–16 October 1987), (b) Lothar, and (c) Martin storms (26–28 December 1999), where red dots indicate the impacted sites.

the considered variable (e.g., waves or surges). A sensitivity analysis is then performed before the application of the method. Thus, it was checked that  $p = 0.99$  can imply the merging of different storms occurring in the same area into a same event. Conversely, with  $p = 0.999$ , a storm can be wrongly separated into two or more events, notably when it loses and regains intensity during its track. Storms are more properly detected when  $p = 0.995$ . Note that the quantile 0.995 was used by Méndez *et al.* [2006] and Ruggiero *et al.* [2010] to estimate extreme wave heights in a POT framework. Figure 2 is a snapshot every 5 h of the area affected by the storm Daria of 24–26 January 1990 (exceedances of the 0.995 quantile).

Moreover, by considering especially the most intense storms, a sensitivity analysis was performed to determine  $(\Delta, \eta)$ , respectively related to the time of wave propagation between two neighboring sites and the density of the grid in Figure 1. The configuration ( $p = 0.995$ ,  $\Delta = 2$  h,  $\eta = 10$ ) is thus chosen, leading to the extraction of 5939 storms. A small descriptive study reveals that, on average: (i) there are 192 storms per year in the study area, with a standard deviation (sd) of 26 storms per year, (ii) a storm impacts 38 sites (sd = 104 sites), and (iii) a storm lasts 12.5 h (sd = 10.3 h) at-site scale.

The map of the at-site 0.995 quantiles of hourly time series of  $H_s$  is given in Figure 3. Footprints of the Great Storm of 1987, Lothar and Martin storms (26–28 December 1999) are presented in Figure 4. Note that both the procedure of extraction of storms and the selected values of  $(p, \Delta, \eta)$  allow the separation of Lothar and Martin which occurred in the same area within 36 h.

### 3.3. Formation of Homogeneous Regions

From the 5939 storms extracted, the criterion of storm propagation (1) is estimated for each pair of sites. Ward's hierarchical classification is then applied on the pairwise dissimilarity indices (2). Figure 5 shows the results for different configurations of storms footprints, when the number of regions  $R$  varies ( $R = 2, 3, 4, 10, 20, 30$ ). It can be seen that the geographical contiguity between sites in a region is naturally obtained, but without forcing it in the algorithm.

The dendrogram of the classification is shown in Figure 6a. The evolution of its standardized heights (Figure 6b) shows a break at five clusters, meaning that a partition into five regions could correspond to the most typical storms footprints. These five physically homogeneous regions are shown in Figure 7: the South Atlantic (region 1, 399 sites), the North Atlantic (region 2, 479 sites), the North Sea (region 3, 241 sites), the English Channel and its approaches (region 4, 392 sites), and the Bay of Biscay (region 5, 336 sites).

Table 1 contains the characterization of these five regions in terms of storm propagation. Specifically, the  $(r, s)$  element of Table 1 is the criterion (1) for two generic sites, respectively, located in region  $r$  and region  $s$ . As can be seen from the diagonal, regions 2 and 5 are, respectively, the least and the most compact, where compactness is characterized by a high probability of storm propagation. Besides, region 1 is the most well separated, meaning that a storm impacting this region is more likely to remain enclosed in this region than a storm in another region. Conversely, region 4 is the least well separated, with permeable boundaries with regions 3 and 5.

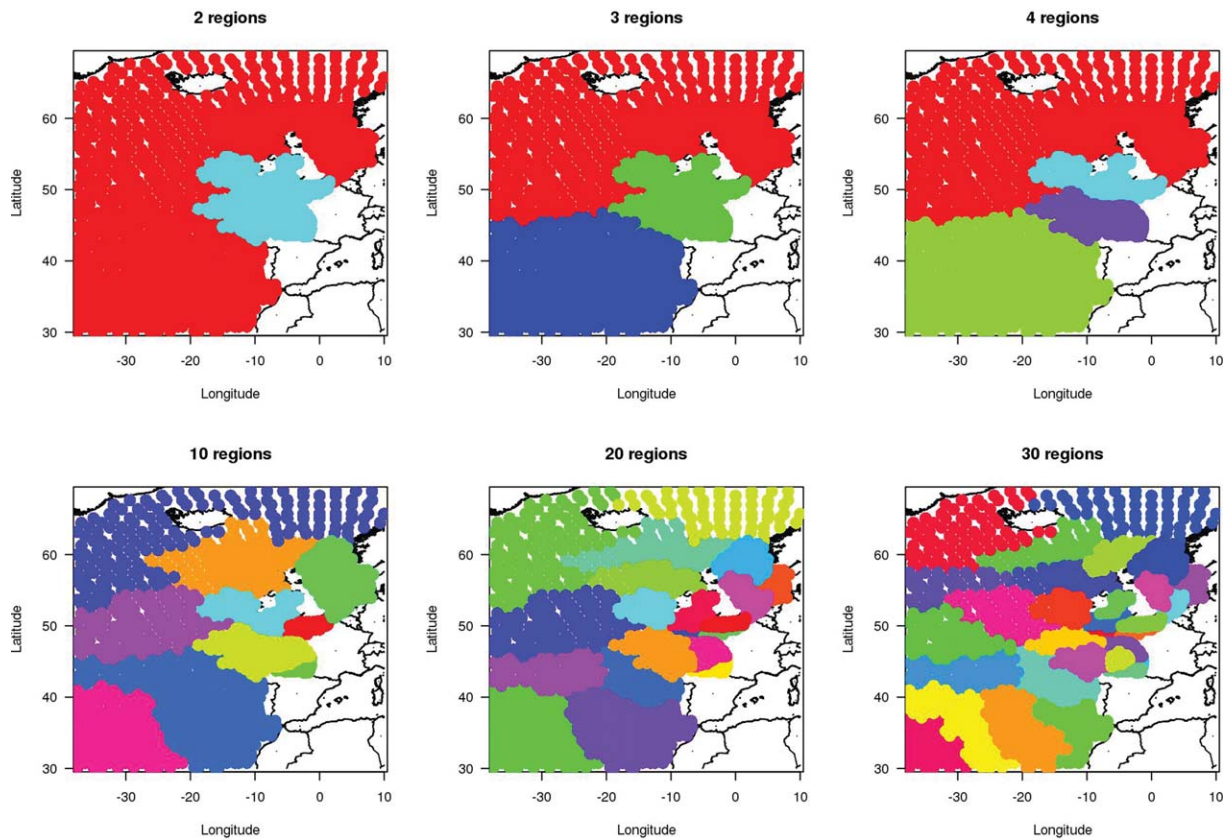


Figure 5. Different configurations of storms footprints from the Ward’s hierarchical classification, for  $R = 2, 3, 4, 10, 20, 30$ .

These five regions present a physical coherence. In particular, each region can be characterized by a specific storminess. First, this can be due to geomorphological aspects. For example, region 3 (North Sea) is a rather closed area. Indeed, Wood *et al.* [2005] classed storm surges impacting the eastern coast of England into three distinct kinds of windstorms specific to North Sea. Moreover, regarding region 4, the corridor

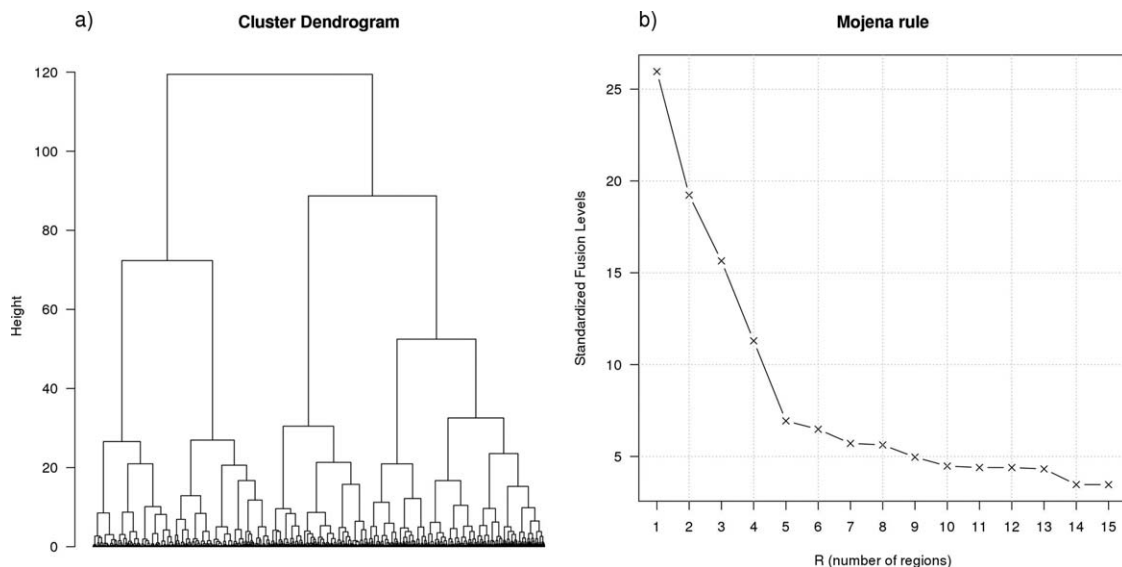


Figure 6. (a) Dendrogram of the classification and (b) evolution of the standardized dendrogram heights.

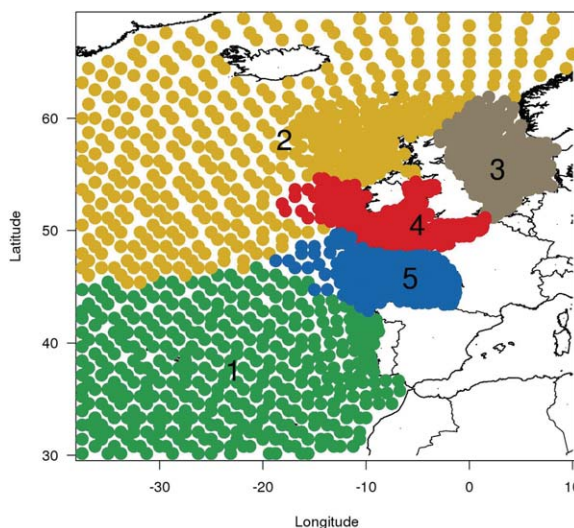


Figure 7. The five regions corresponding to the most typical storms footprints.

Table 1. Distance Between Regions in Terms of  $p_{ij}$ <sup>a</sup>

Region	1	2	3	4	5
1	0.26	0.03	0.01	0.03	0.08
2	0.03	0.15	0.05	0.07	0.04
3	0.01	0.05	0.28	0.11	0.05
4	0.03	0.07	0.11	0.36	0.20
5	0.08	0.04	0.05	0.20	0.44

<sup>a</sup>The  $(r,s)$  element of this matrix is the mean value of  $p_{ij}$  for site  $i$  located in region  $r$ , and for site  $j$  located in region  $s$ .

Azores high, are associated with northeastward storm tracks above 50°N, in the area of region 2. As for negative phases of the NAO, they are related to weaker southward-shifted winds, notably in region 1. Moreover, during positive phases of the East Atlantic (EA) pattern, storms occur at lower latitudes than in positive NAO phases, between 35° and 50°N (region 1). A positive phase of the East Atlantic/Western Russia (EA/WR) pattern is, for its part, associated with decreased storminess in the Bay of Biscay (region 5), while the storminess

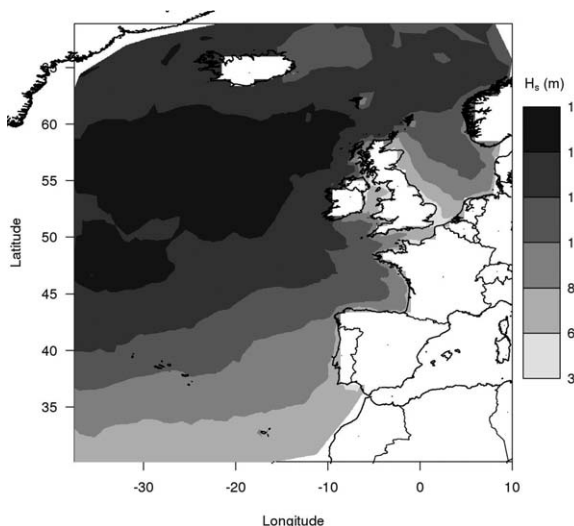
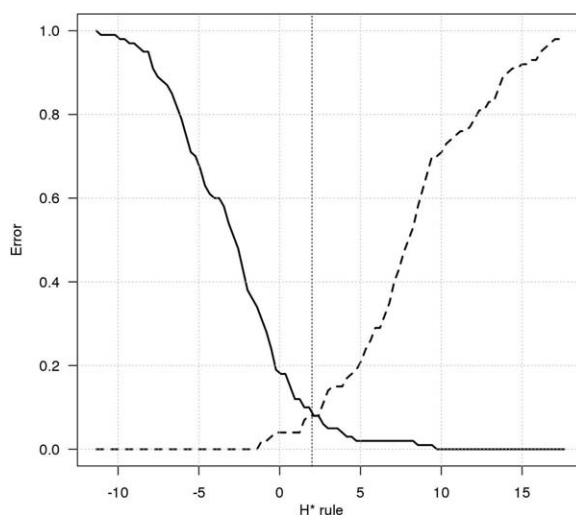


Figure 8. Map of threshold values of  $H_s$  exceeded on average once per year (m).

configuration of the English Channel represents a suggested pathway for storms [Tonnerre-Guerin, 2003]. Second, climatological considerations are relevant to justify the five regions. In particular, the analysis of the domain of influence of teleconnection patterns allows identifying regions which are quite similar to the obtained partition. Teleconnection patterns are indices describing the large-scale atmospheric conditions. They are relevant to explain northern Atlantic storminess variability [Seierstad et al., 2007]. Izaguirre et al. [2010] showed their influence on the interannual variability of the extreme wave climate in the North-East Atlantic; Le Cozannet et al. [2011] related the variability of sea-wave states in the Bay of Biscay to teleconnection patterns. According to Le Cozannet et al. [2011] and Seierstad et al. [2007], positive phases of the North Atlantic Oscillation (NAO), characterized by a deep Icelandic low and a more intense Icelandic high, are associated with northeastward storm tracks above 50°N, in the area of region 2. As for negative phases of the NAO, they are related to weaker southward-shifted winds, notably in region 1. Moreover, during positive phases of the East Atlantic (EA) pattern, storms occur at lower latitudes than in positive NAO phases, between 35° and 50°N (region 1). A positive phase of the East Atlantic/Western Russia (EA/WR) pattern is, for its part, associated with decreased storminess in the Bay of Biscay (region 5), while the storminess is increased in the central part of North Atlantic. Finally, positive phases of the East Pacific/North Pacific (EP/NP) pattern increase the storminess in the Bay of Biscay (region 5).

### 3.4. Preparation of Samples for Statistical Analysis

The statistical redefinition of storms described in section 2.3 is performed in such a way that there is  $\lambda = 1$  storm per year on average at each site. This leads to retain 1340 storms among the 5939. It has been checked that the choice  $\lambda = 1$  corresponds to thresholds higher than  $q_{0.995}$ , the 0.995 quantiles of hourly time series of  $H_s$ . Site  $i$  is therefore



**Figure 9.** Statistical homogeneity testing in the presence of intersite dependence: Monte Carlo type I error (solid line) and type II error (dotted line) as a function of the  $H^*$  rule (cut-off value above which homogeneity is rejected).

characterized by the sample of  $H_s$  over the threshold  $u_i$  exceeded on average once per year; the sample size is 31, as 31 years of data are available. These thresholds, which are also the local indices used for RFA, are represented in Figure 8.

### 3.5. Intersite Dependence Effects in Testing the Statistical Homogeneity

The five obtained regions correspond to typical storms footprints. Therefore, a strong intersite dependence can be expected inside a given region, and this may affect the performances of the  $H = 2$  criterion defined in section 2.4 to test the statistical homogeneity. This thus

section investigates the validity of this criterion to detect heterogeneity in large regions with a high degree of intersite dependence.

Hosking and Wallis [1997, Table 6.1] present a convenient way to simulate synthetic regions with a given degree of intersite correlation. Here simulations are based on region 1: each synthetic region has 399 sites, with an intersite correlation structure equivalent to the one of region 1. Note that, unlike the annual maxima framework, the correlation between two sites is not straightforward to assess for POT data, especially due to the difficulty to properly define the temporal simultaneity of the observations at two different sites. Thus, intersite dependence of POT data was expressed through the pairwise correlations of annual maxima series. Note that annual maxima series can be easily extracted from the 5939 storms, as these storms generally provide at least one value per year (which may not be the case after their statistical redefinition leading to 1340 storms). Then, correlation  $\rho_{ij}$  between sites  $i$  and  $j$  is modeled by  $\rho_{ij} = \exp(-\beta d_{ij})$  where  $d_{ij}$  is the distance between  $i$  and  $j$ . From the empirical pairwise correlation coefficients in region 1,  $\beta$  is estimated by nonlinear least squares at  $9.5 \times 10^{-4}$ , meaning that, for example,  $\rho_{ij} = 0.62$  for two sites distant from 500 km.

In a synthetic homogeneous region, data at site  $i$  are sampled from the  $GPD(u_i, \gamma u_i, k)$ , where  $u_i$  is the local index found in section 3.4 and  $(\gamma, k)$  are the estimated regional GPD parameters in region 1 ( $\gamma = 0.159$  and  $k = -0.015$ , see section 3.7). Besides, heterogeneity is defined as follows: at-site GPD shape parameters linearly vary in  $[k - 0.2, k + 0.2]$ , where  $k = -0.015$ .

Hundred homogeneous regions and 100 heterogeneous regions are thus simulated (with the specified model of intersite dependence), and the  $H$  statistic is computed for each of them. This procedure allows to estimate a Monte Carlo type I error (probability to declare heterogeneous a homogeneous region) and type II error (probability to declare homogeneous a heterogeneous region) for testing the statistical homogeneity, depending on a given  $H^*$  rule (cutoff value above which homogeneity is rejected). Figure 9 shows the evolution of these two types of error depending on the  $H^*$  rule. As expected, the type I error decreases with  $H^*$  and the type II error increases with  $H^*$ . Moreover, the cutoff value  $H^* = 2$  implies relatively low values of these two errors (type I error = 0.10 and type II error = 0.08). Thus, even if the region is large with a strong intersite dependence, the criterion  $H^* = 2$  remains valid to test its statistical homogeneity.

### 3.6. Statistical Homogeneity of the Obtained Regions

The procedure of section 2.4 is here applied to get both physically and statistically

**Table 2.** Heterogeneity Measure  $H$  for Each of the Five Regions

Region	1	2	3	4	5
H	1.60	-0.07	-2.36	4.22	7.36

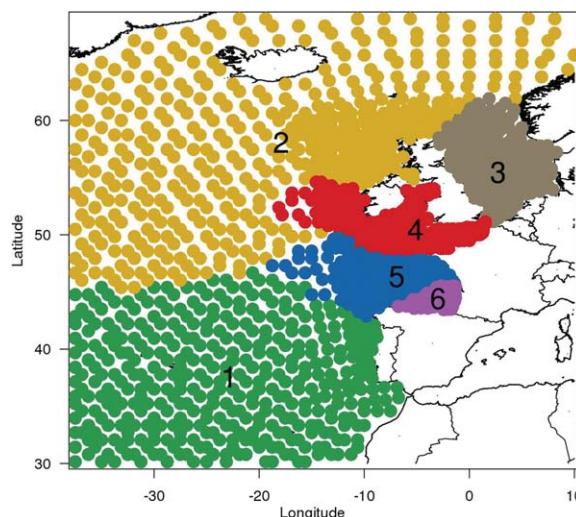


Figure 10. Proposed division into six physically and statistically homogeneous regions.

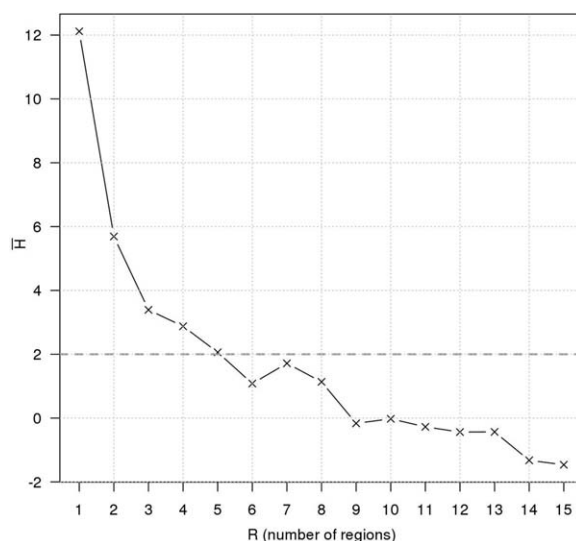


Figure 11. Mean value of  $H$  in the study area as a function of  $R$ . The dashed line corresponds to the threshold of heterogeneity  $H = 2$ .

homogeneous regions. The heterogeneity measure  $H$  is computed for each of the five regions (Table 2). Regions 1, 2, and 3 can be viewed as statistically homogeneous. However, heterogeneities are contained in regions 4 and 5. These regions cannot be accepted and have to be redefined before performing a RFA.

Fifteen sites among the 392 from region 4 are statistically discordant. When these sites are removed, the region is statistically homogeneous ( $H = 0.68$ ). These discordant sites (which do not form a homogeneous region themselves) are actually located near the coasts, where local effects can highly influence extreme  $H_s$ . From now on, the Channel region is restricted to the 377 nondiscordant sites.

Regarding region 5, removing discordant sites does not help to improve its statistical homogeneity. It is therefore subdivided into the two inner storms footprints implied by the clustering hierarchy: North ( $H = -0.45$ , 234 sites) and South ( $H = -4.69$ , 102 sites) of Bay of Biscay. These new regions are statistically homogeneous. In particular, stronger statistical asymmetries are found in the data from the South of Bay of Biscay, which can justify this subdivision.

Six regions, both physically and statistically homogeneous, are therefore detected, allowing the estimation of extreme quantiles through RFA. These regions are represented in Figure 10. Note that 6, 13, 6, 12, 6, and 6 discordant sites ( $D > 3$ ) are, respectively, found for each of the six homogeneous regions. Most of them are coastal sites, but are far from each other and there are no gross errors in their data: they are thus left inside their regions.

Finally, the proposed method allows increasing the overall statistical homogeneity. Indeed, the whole area is highly statistically heterogeneous ( $H = 12.12$ ), underlining the interest of a subdivision into smaller regions on a physical basis. Figure 11 represents the mean value of  $H$  in the study area as a function of  $R$ ; it can be seen that the finer are the storms footprints, the more improved is the statistical homogeneity.

### 3.7. Estimation of Extreme Significant Wave Heights Through RFA

Note that the results presented here should be seen as a possible application of the proposed method to form homogeneous regions, rather than a tool or results to use in the design of marine structures, especially in coastal areas. Indeed, the present analysis uses data from the oceanic model of ANEMOC-2, whose resolution is not sufficient in coastal areas and which includes only parts of the shallow-water effects. For these

**Table 3.** Regional Parameters:  $\gamma$  (GPD Scale Parameter),  $k$  (GPD Shape Parameter),  $y_{0.99}$  (100 Year Regional Return Level)

Region	1	2	3	4	5	6
$\gamma$	0.159	0.133	0.137	0.140	0.143	0.141
$k$	-0.015	0.023	-0.002	0.142	-0.033	0.218
$y_{0.99}$	1.707	1.646	1.627	1.909	1.611	2.119

reasons, estimates for coastal areas are not shown in this section. Note this oceanic model is supplemented by a coastal one, whose resolution is finer on the continental shelf, in the Channel and along the French coast. In a follow-up of this study, data from the coastal model of ANEMOC-2 may improve the simulated seas-states in coastal areas.

For each of the six homogeneous regions, the regional GPD parameters ( $\gamma$ ,  $k$ ) are estimated following the procedure presented in section 2.5. These quantities are given in Table 3, as well as the 100 year regional return level  $y_{0.99}$ . The shape parameter  $k$  is positive (corresponding to an unbounded GPD) in regions 2, 4 and 6, suggesting a higher intensity of extreme  $H_s$ . Besides, a regional  $L$ -moment ratio diagram (not shown) proves that the GPD provides an adequate fit to the data, compared to other distributions.

At-site return levels are obtained by multiplying regional return levels by the local indices. Return levels plot for six sites located in each region are provided in Figure 12. Moreover, Figure 13 shows the map of the estimated at-site 100 year  $H_s$ . They display a coherent spatial pattern, with lower values near the West European coasts. The highest return levels are obtained for sites located in the north-central part of the study area (up to about 29 m). These estimates are comparable to those from *Caires and Sterl* [2005, Figure 10] based on ERA-40 reanalysis data. Although slightly higher values are here found in the area of the largest estimates, their spatial structure is indeed essentially similar. Besides, note that there is no apparent discontinuity effect in the spatial variation of the estimated 100 year  $H_s$ , which would be due to the fixed nature of

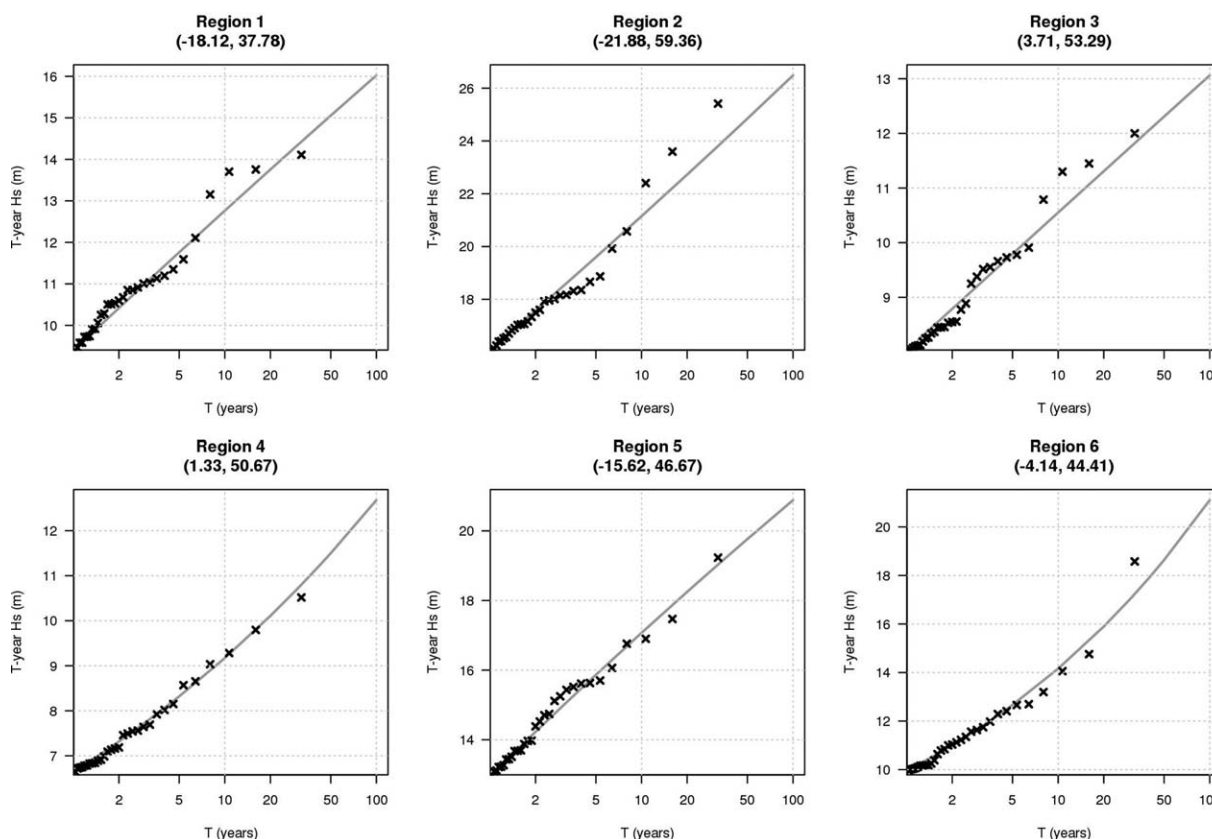


**Figure 12.** Return levels plot for six sites located in each region (crosses represent at-site ANEMOC-2 results). Coordinates are denoted (longitude and latitude) in degrees.

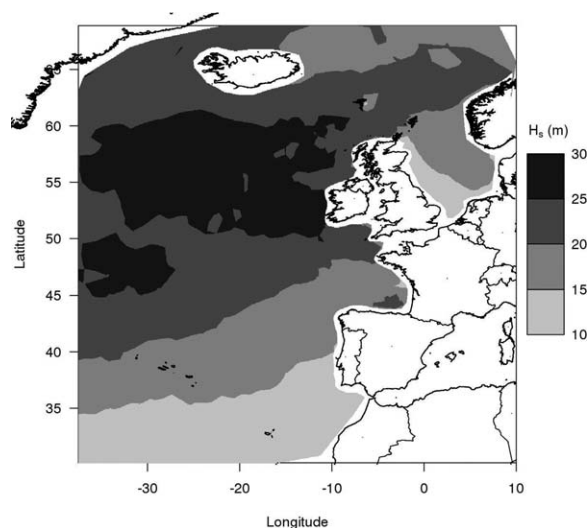


Figure 13. Map of estimated 100 year  $H_s$  (m).

regions. Indeed, they are spatially smooth, even in the areas located near the boundaries of the homogeneous regions.

#### 4. Conclusions

Compared to a local statistical analysis of extremes, RFA can reduce uncertainties in the estimations of return levels, provided that homogeneous regions can be delineated. In the framework of extreme marine events, a method to form homogeneous regions by identifying typical storms footprints is proposed in this paper.

First, a spatiotemporal declustering procedure is employed to detect storms generating marine extremes. Gathering extremes neighbors in space and time, a careful attention is paid to ensure their proper reconstitution. In particular, different storms taking place simultaneously in different areas can be distinguished, as well as storms successively occurring in the same zone, e.g., the Lothar and Martin storms of December 1999.

Second, the identification of the most typical storms footprints in the study area relies on the Ward's hierarchical clustering based on a criterion of storm propagation. These physically homogeneous regions are readily explicable. Indeed, sites from a given region are likely to be impacted by the same storms, and any storm impacting a region is likely to remain enclosed in this region. This procedure is fairly simple to implement, as the only information required is the time of occurrence of the observed extremes.

An application to the estimation of extreme significant wave heights from the numerical sea-state database ANEMOC-2 is given. Six regions, both physically and statistically homogeneous, are delineated in the North-East part of the Atlantic Ocean. The geographical contiguity between sites in a region is naturally obtained. It is also shown that the identification of storms footprints allows the increase of the overall regions' statistical homogeneity. Combined with RFA, the proposed method highlights regional differences in the spatial extent and intensity of storms.

Although the proposed example is focused on significant wave heights, the method can easily be applied to other marine variables. Indeed, it is variable-oriented, in the sense that the identified storms footprints are specific to the variable of interest. Moreover, it can deal with cases where periods of observations are not the same for all sites, and/or in the presence of missing data.

Compared to the traditional statistical approaches to form homogeneous regions, the proposed methodology distinguishes physical considerations from statistical ones. First, regions are delineated from a physical basis; second, their statistical homogeneity is checked. Note that (i) hierarchical clustering provides here a natural way to subdivide heterogeneous regions in order to increase homogeneity and (ii) the method is shown to be robust to intersite dependence inherent to regions delineated as storms footprints. It would be possible, however, to form regions in one step: for example, the Ward's clustering algorithm could be modified to also involve the statistical homogeneity of the regions, but without concealing the criterion of storm propagation.

By providing information on the spatiotemporal extension of the observed extremes, the storms defined in this paper may be used in a broader framework than RFA. In particular, several studies dealing with spatial extremes are based on the analysis of block maxima series observed in space; for instance, Bernard *et al.* [2013] partitioned French sites into five regions according to the strength of dependence of weekly precipitation maxima. However, block maxima series observed at two different sites may be highly dependent but they might not have

occurred simultaneously during the same physical events. Conversely, relying on the storms allows reasoning on the scale of the physical events, offering a proper framework to model spatial extremes.

Looking forward future improvements, the formation of homogeneous regions would surely benefit from other physical considerations complementary to the storms footprints, such as the water depth. For example, the statistical heterogeneity of region 5 (see Figure 7) might come from the fact that this is the only region not homogeneous in water depth. Indeed, regions 1 and 2 correspond to deep water and regions 3 and 4 to the continental shelf. Moreover, the procedure of identification of storms footprints should be compared to a similar study based on meteorological conditions generating marine extremes (atmospheric pressure and wind fields).

Future works could also deal with intersite dependence when estimating extremes. Indeed, as sites in a region are likely to be impacted by the same physical events, regions are expected to display a strong intersite dependence. Although ignored in the estimation process because of the robust nature of the regional  $L$ -moments method against intersite dependence, taking it into account could improve the reliability of extrapolations.

#### Acknowledgments

The permission to publish the results of this ongoing research study was granted by the Electricité de France (EDF) company. The results in this paper should, of course, be considered as R&D exercises without any significance or embedded commitments upon the real behavior of the EDF power facilities or its regulatory control and licensing. The authors would like to thank Amélie Laugel who kindly provided the ANEMOC-2 data used in this study, and the three anonymous reviewers who improved this paper by their constructive comments and suggestions. The wave data set used for the analyses presented in this article has been extracted from the ANEMOC-2 database. This data set can be obtained by request addressed to the corresponding author. The use of this data is restricted to research purpose, all industrial or commercial applications being excluded.

#### References

- Anderson, C. W., D. J. T. Carter, and P. D. Cotton (2001), Wave climate variability and impact on offshore design extremes, report commissioned from the University of Sheffield and Satellite Observing Systems for Shell International and the Organization of Oil & Gas Producers, London, 99 pp.
- Bardet, L., C.-M. Duluc, V. Rebour, and J. L'Her (2011), Regional frequency analysis of extreme storm surges along the French coast, *Nat. Hazards Earth Syst. Sci.*, 11(6), 1627–1639.
- Beable, M. E., and A. I. McKerchar (1982), Regional flood estimation in New Zealand, *Tech. Rep. 20*, 132 pp., Water and Soil Div., Ministry of Works and Development, Wellington.
- Benoit, M., F. Marcos, and F. Becq (1996), Development of a third generation shallow-water wave model with unstructured spatial meshing, in *Proceedings of the 25th International Conference on Coastal Engineering*, pp. 465–478, American Society of Civil Engineers (ASCE), Orlando, Florida.
- Bernard, E., P. Naveau, M. Vrac, and O. Mestre (2013), Clustering of maxima: Spatial dependencies among heavy rainfall in France, *J. Clim.*, 26, 7929–7937.
- Bernardara, P., M. Andreewsky, and M. Benoit (2011), Application of the Regional Frequency Analysis to the estimation of extreme storm surges, *J. Geophys. Res.*, 116, C02008, doi:10.1029/2010JC006229.
- Bernardara, P., F. Mazas, X. Kergadallan, and L. Hamm (2014), A two-step framework for over-threshold modelling of environmental extremes, *Nat. Hazards Earth Syst. Sci.*, 14, 635–647.
- Betts, N. L., J. D. Orford, D. White, and C. J. Graham (2004), Storminess and surges in the South-Western approaches of the Eastern North Atlantic: The synoptic climatology of recent extreme coastal storms, *Mar. Geol.*, 210(1–4), 227–246.
- Blashfield, R. K. (1976), Mixture model tests of cluster analysis: Accuracy of four agglomerative hierarchical methods, *Psychol. Bull.*, 83(3), 377–388.
- Butler, A. (2005), Statistical modelling of synthetic oceanographic extremes, PhD thesis, Lancaster Univ., Lancaster, U. K.
- Caires, S., and A. Sterl (2005), 100-year return value estimates for ocean wind speed and significant wave height from the ERA-40 data, *J. Clim.*, 18(7), 1032–1048.
- Cao, Y., A. W. Bark, and W. P. Williams (1997), A comparison of clustering methods for river benthic community analysis, *Hydrobiologia*, 347, 25–40.
- Casson, E., and S. Coles (1999), Spatial regression models for extremes, *Extremes*, 1(4), 449–468.
- Darlymple, T. (1960), Flood frequency analysis, *U.S. Geol. Surv. Water Supply Pap.*, 1543-A.
- Davison, A. C., S. A. Padoan, and M. Ribatet (2012), Statistical modeling of spatial extremes, *Stat. Sci.*, 27(2), 161–186.
- Everitt, B. S., and G. Dunn (2001), *Applied Multivariate Data Analysis*, 2nd ed., Oxford Univ. Press, New York.
- Ferreira, L., and D. B. Hitchcock (2009), A comparison of hierarchical methods for clustering functional data, *Commun. Stat.*, 38(9), 1925–1949.
- Gabriele, S., and F. Chiaravalloti (2013), Using the meteorological information for the regional rainfall frequency analysis: An application to Sicily, *Water Resour. Manage.*, 27(6), 1721–1735.
- Gingras, D., K. Adamowski, and P. J. Pilon (1994), Regional flood equations for the provinces of Ontario and Quebec, *Water Resour. Bull.*, 30, 55–67.
- Goda, Y. (2011), Plotting-position estimator for the L-moment method and quantile confidence interval for the GEV, GPA, and Weibull distributions applied for extreme wave analysis, *Coastal Eng.*, 53(2), 111–149.
- Goda, Y., M. Kudaka, and H. Kawai (2010), Incorporating of Weibull distribution in L-moments method for regional frequency analysis of peak over threshold wave heights, in *Proceedings of the 32th International Conference on Coastal Engineering*, American Society of Civil Engineers (ASCE), Shanghai, China.
- Holt, T. (1999), A classification of ambient climatic conditions during extreme surge events off Western Europe, *Int. J. Climatol.*, 19(7), 725–744.
- Hosking, J. R. M. (2012), Towards statistical modeling of tsunami occurrence with regional frequency analysis, *J. Math. Ind.*, 4(2012A-6), 41–48.
- Hosking, J. R. M., and J. R. Wallis (1988), The effect of intersite dependence on regional flood frequency analysis, *Water Resour. Res.*, 24(4), 588–600.
- Hosking, J. R. M., and J. R. Wallis (1993), Some statistics useful in regional frequency analysis, *Water Resour. Res.*, 29(2), 271–281.
- Hosking, J. R. M., and J. R. Wallis (1997), *Regional Frequency Analysis: An Approach Based on L-Moments*, Cambridge Univ. Press, Cambridge, U. K.
- Izaguirre, C., F. J. Méndez, M. Menendez, A. Luceno, and I. J. Losada (2010), Extreme wave climate variability in southern Europe using satellite data, *J. Geophys. Res.*, 115, C04009, doi:10.1029/2009JC005802.
- Kalkstein, L. S., T. Guanri, and J. A. Skindlov (1987), An evaluation of three clustering procedures for use in synoptic climatological classification, *J. Clim. Appl. Meteorol.*, 26, 717–730.

- Kergadallan, X. (2013), *Analyse statistique des niveaux d'eau extrêmes—Environnements maritime et estuarien*, 179 p., CETMEF, Centre d'études techniques maritimes et fluviales, Compiègne, France.
- Laugel, A. (2013), Sea state climatology in the North-East Atlantic Ocean: Analysis of the present climate and future evolutions under climate change scenarios by means of dynamical and statistical downscaling methods, PhD thesis, EDF R&D LNHE, Saint-Venant Lab. for Hydraul., Chatou, France.
- Leckebusch, G. C., D. Renggli, and U. Ulbrich (2008), Development and application of an objective storm severity measure for the Northeast Atlantic region, *Meteorol. Z.*, *17*(5), 575–587.
- Le Cozannet, G., S. Lecacheux, E. Delvallee, N. Desramaut, C. Oliveros, and R. Pedreros (2011), Teleconnection pattern influence on sea-wave climate in the Bay of Biscay, *J. Clim.*, *24*, 641–652.
- Mailier, P. J., D. B. Stephenson, C. A. T. Ferro, and K. I. Hodges (2006), Serial clustering of extratropical cyclones, *Mon. Weather Rev.*, *134*, 2224–2240.
- Martinez, W. L., and A. R. Martinez (2004), *Exploratory Data Analysis With MATLAB*, Chapman and Hall/CRC, Boca Raton.
- Méndez, F. J., M. Menéndez, A. Luceño, and I. J. Losada (2006), Estimation of the long-term variability of extreme significant wave height using a time-dependent Peak Over Threshold (POT) model, *J. Geophys. Res.*, *111*, C07024, doi:10.1029/2005JC003344.
- Michelangeli, P. A., R. Vautard, and B. Legras (1995), Weather regimes: Recurrence and quasi stationarity, *J. Atmos. Sci.*, *52*, 1237–1256.
- Mirkin, B. (2005), *Clustering for Data Mining: A Data Recovery Approach*, Chapman and Hall/CRC, Boca Raton.
- Modarres, R., and A. Sarhadi (2011), Statistically-based regionalization of rainfall climates of Iran, *Global Planet. Change*, *75*(1–2), 67–75.
- Mojena, R. (1977), Hierarchical grouping methods and stopping rules: An evaluation, *Comput. J.*, *20*, 359–363.
- Morin, G., J. P. Fortin, W. Sochanska, J. P. Lardeau, and R. Charbonneau (1979), Use of principal component analysis to identify homogeneous precipitation stations for optimal interpolation, *Water Resour. Res.*, *15*(6), 1841–1850.
- Nissen, K. M., G. C. Leckebusch, J. G. Pinto, D. Renggli, S. Ulbrich, and U. Ulbrich (2010), Cyclones causing wind storms in the Mediterranean: Characteristics, trends and links to largescale patterns, *Nat. Hazards Earth Syst. Sci.*, *10*, 1379–1391.
- Onibon, H., T. B. M. J. Ouarda, M. Barbet, A. St Hilaire, B. Bobee, and P. Bruneau (2004), Regional frequency analysis of annual maximum daily precipitation in Quebec, Canada, *Hydrol. Sci. J.*, *49*(4), 717–735.
- Pickands, J. (1975), Statistical inference using extreme order statistics, *Ann. Stat.*, *3*(1), 119–131.
- Ramachandra Rao, A., and V. V. Srinivas (2006), Regionalization of watersheds by hybrid-cluster analysis, *J. Hydrol.*, *318*(1–4), 37–56.
- Renggli, D., G. C. Leckebusch, U. Ulbrich, S. N. Gleixner, and E. Faust (2011), The skill of seasonal ensemble prediction systems to forecast wintertime windstorm frequency over the North Atlantic and Europe, *Mon. Weather Rev.*, *139*, 3052–3068.
- Rosbjerg, D. (1985), Estimation in partial duration series with independent and dependent peak values, *J. Hydrol.*, *76*, 183–195.
- Roth, M., T. Buishand A., Jongbloed, G., Klein Tank, A. M. G. and J. H. van Zanten (2012), A regional peaks-over-threshold model in a nonstationary climate, *Water Resour. Res.*, *48*, W11533, doi:10.1029/2012WR012214.
- Ruggiero, P., P. D. Komar, and J. C. Allan (2010), Increasing wave heights and extreme value projections: The wave climate of the U.S. Pacific Northwest, *Coastal Eng.*, *57*(5), 539–552.
- Saha, S., et al. (2010), The NCEP climate forecast system reanalysis, *Bull. Am. Meteorol. Soc.*, *91*, 1015–1057.
- Satyanarayana, P., and V. V. Srinivas (2008), Regional frequency analysis of precipitation using large-scale atmospheric variables, *J. Geophys. Res.*, *113*, D24110, doi:10.1029/2008JD010412.
- Seierstad, I. A., D. B. Stephenson, and N. G. Kvamsto (2007), How useful are teleconnection patterns for explaining variability in extratropical storminess?, *Tellus, Ser. A*, *59*(2), 170–181.
- Tonnerre-Guerin, M. A. (2003), Les tempêtes, un concept et une genèse revisités: l'exemple de la façade occidentale de l'Europe, *Ann. Géogr.*, *112*(633), 451–470.
- Ulbrich, U., G. C. Leckebusch, and J. G. Pinto (2009), Extra-tropical cyclones in the present and future climate: A review, *Theor. Appl. Climatol.*, *96*(1–2), 117–131.
- Van Gelder, P. H. A. J. M., and N. M. Neykov (1998), Regional frequency analysis of extreme water levels along the Dutch Coast using L-moments: A preliminary study, in *International Scientific Conference on Stochastic Models of Hydrological Processes and Their Application to Problems of Environmental Preservation*, NATO, Advanced Research Workshop, pp. 14–20, Moscow, Russia.
- Van Gelder, P. H. A. J. M., J. De Ronde, N. M. Neykov and P. Neytchev (2000), Regional frequency analysis of extreme wave heights: Trading space for time, in *Proceedings of the 27th International Conference on Coastal Engineering*, American Society of Civil Engineers (ASCE), Sydney, pp. 1099–1112, NSW, Australia.
- Ward, J. (1963), Hierarchical grouping to optimize an objective function, *J. Am. Stat. Assoc.*, *58*, 236–244.
- Weiss, J., and P. Bernardara (2013), Comparison of local indices for regional frequency analysis with an application to extreme skew surges, *Water Resour. Res.*, *49*, 2940–2951.
- Wood, R. M., M. Drayton, A. Berger, P. Burgess, and T. Wright (2005), Catastrophe loss modelling of storm-surge flood risk in eastern England, *Philos. Trans. R. Soc. A*, *363*, 1407–1422.
- Yun, E. K., and S. B. Cho (2006), Adaptive fingerprint image enhancement with fingerprint image quality analysis, *Image Vision Comput.*, *24*, 101–110.